Measurement of the *W* Boson Mass with the D0 Detector

V. M. Abazov,[32] B. Abbott,[70] B. S. Acharya,[26] M. Adams,[46] T. Adams,[44] G. D. Alexeev,[32] G. Alkhazov,[36] A. Alton,[58,†] G. Alverson,[57] M. Aoki,[45] A. Askew,[44] B. Åsman,[38] S. Atkins,[55] O. Atramentov,[62] K. Augsten,[7] C. Avila,[5] F. Badaud,[10] L. Bagby,[45] B. Baldin,[45] D. V. Bandurin,[44] S. Banerjee,[26] E. Barberis,[57] P. Baringer,[53] J. Barreto,[2] J. F. Bartlett,[45] U. Bassler,[15] V. Bazterra,[46] A. Bean,[53] M. Begalli,[2] C. Belanger-Champagne,[38] L. Bellantoni,[45] S. B. Beri,[24] G. Bernardi,[14] R. Bernhard,[19] I. Bertram,[39] M. Besançon,[15] R. Beuselinck,[40] V. A. Bezzubov,[35] P. C. Bhat,[45] S. Bhatia,[60] V. Bhatnagar,[24] G. Blazey,[47] S. Blessing,[44] K. Bloom,[61] A. Boehnlein,[45] D. Boline,[67] E. E. Boos,[34] G. Borissov,[39] T. Bose,[56] A. Brandt,[73] O. Brandt,[20] R. Brock,[59] G. Brooijmans,[65] A. Bross,[45] D. Brown,[14] J. Brown,[14] X. B. Bu,[45] M. Buehler,[45] V. Buescher,[21] V. Bunichev,[34] S. Burdin,[39,‡] C. P. Buszello,[38] E. Camacho-Pérez,[29] B. C. K. Casey,[45] H. Castilla-Valdez,[29] S. Caughron,[59] S. Chakrabarti,[67] D. Chakraborty,[47] K. M. Chan,[51] A. Chandra,[75] E. Chapon,[15] G. Chen,[53] S. Chevalier-Théry,[15] D. K. Cho,[72] S. W. Cho,[28] S. Choi,[28] B. Choudhary,[25] S. Cihangir,[45] D. Claes,[61] J. Clutter,[53] M. Cooke,[45] W. E. Cooper,[45] M. Corcoran,[75] F. Couderc,[15] M.-C. Cousinou,[12] A. Croc,[15] D. Cutts,[72] A. Das,[42] G. Davies,[40] S. J. de Jong,[30,31] E. De La Cruz-Burelo,[29] F. Déliot,[15] R. Demina,[66] D. Denisov,[45] S. P. Denisov,[35] S. Desai,[45] C. Deterre,[15] K. DeVaughan,[61] H. T. Diehl,[45] M. Diesburg,[45] P. F. Ding,[41] A. Dominguez,[61] T. Dorland,[77] A. Dubey,[25] L. V. Dudko,[34] D. Duggan,[62] A. Duperrin,[12] S. Dutt,[24] A. Dyshkant,[47] M. Eads,[61] D. Edmunds,[59] J. Ellison,[43] V. D. Elvira,[45] Y. Enari,[14] H. Evans,[49] A. Evdokimov,[68] V. N. Evdokimov,[35] G. Facini,[57] L. Feng,[47] T. Ferbel,[66] F. Fiedler,[21] F. Filthaut,[30,31] W. Fisher,[59] H. E. Fisk,[45] M. Fortner,[47] H. Fox,[39] S. Fuess,[45] A. Garcia-Bellido,[66] G. A. García-Guerra,[29,§] V. Gavrilov,[33] P. Gay,[10] W. Geng,[12,59] D. Gerbaudo,[63] C. E. Gerber,[46] Y. Gershtein,[62] G. Ginther,[45,66] G. Golovanov,[32] A. Goussiou,[77] P. D. Grannis,[67] S. Greder,[16] H. Greenlee,[45] G. Grenier,[17] Ph. Gris,[10] J.-F. Grivaz,[13] A. Grohsjean,[15,‖] S. Grünendahl,[45] M. W. Grünewald,[27] T. Guillemin,[13] G. Gutierrez,[45] P. Gutierrez,[70] A. Haas,[65,¶] S. Hagopian,[44] J. Haley,[57] L. Han,[4] K. Harder,[41] A. Harel,[66] J. M. Hauptman,[52] J. Hays,[40] T. Head,[41] T. Hebbeker,[18] D. Hedin,[47] H. Hegab,[71] A. P. Heinson,[43] U. Heintz,[72] C. Hensel,[20] I. Heredia-De La Cruz,[29] K. Herner,[58] G. Hesketh,[41,**] M. D. Hildreth,[51] R. Hirosky,[76] T. Hoang,[44] J. D. Hobbs,[67] B. Hoeneisen,[9] M. Hohlfeld,[21] I. Howley,[73] Z. Hubacek,[7,15] V. Hynek,[7] I. Iashvili,[64] Y. Ilchenko,[74] R. Illingworth,[45] A. S. Ito,[45] S. Jabeen,[72] M. Jaffré,[13] A. Jayasinghe,[70] R. Jesik,[40] K. Johns,[42] E. Johnson,[59] M. Johnson,[45] A. Jonckheere,[45] P. Jonsson,[40] J. Joshi,[24] A. W. Jung,[45] A. Juste,[37] K. Kaadze,[54] E. Kajfasz,[12] D. Karmanov,[34] P. A. Kasper,[45] I. Katsanos,[61] R. Kehoe,[74] S. Kermiche,[12] N. Khalatyan,[45] A. Khanov,[71] A. Kharchilava,[64] Y. N. Kharzheev,[32] J. M. Kohli,[24] A. V. Kozelov,[35] J. Kraus,[59] S. Kulikov,[35] A. Kumar,[64] A. Kupco,[8] T. Kurča,[17] V. A. Kuzmin,[34] S. Lammers,[49] G. Landsberg,[72] P. Lebrun,[17] H. S. Lee,[28] S. W. Lee,[52] W. M. Lee,[45] J. Lellouch,[14] H. Li,[11] L. Li,[43] Q. Z. Li,[45] J. K. Lim,[28] D. Lincoln,[45] J. Linnemann,[59] V. V. Lipaev,[35] R. Lipton,[45] H. Liu,[74] Y. Liu,[4] A. Lobodenko,[36] M. Lokajicek,[8] R. Lopes de Sa,[67] H. J. Lubatti,[77] R. Luna-Garcia,[29,††] A. L. Lyon,[45] A. K. A. Maciel,[1] R. Madar,[15] R. Magaña-Villalba,[29] S. Malik,[61] V. L. Malyshev,[32] Y. Maravin,[54] J. Martínez-Ortega,[29] R. McCarthy,[67] C. L. McGivern,[53] M. M. Meijer,[30,31] A. Melnitchouk,[60] D. Menezes,[47] P. G. Mercadante,[3] M. Merkin,[34] A. Meyer,[18] J. Meyer,[20] F. Miconi,[16] N. K. Mondal,[26] H. E. Montgomery,[45,‡‡] M. Mulhearn,[76] E. Nagy,[12] M. Naimuddin,[25] M. Narain,[72] R. Nayyar,[42] H. A. Neal,[58] J. P. Negret,[5] P. Neustroev,[36] T. Nunnemann,[22] G. Obrant,[36,*] J. Orduna,[75] N. Osman,[12] J. Osta,[51] M. Padilla,[43] A. Pal,[73] N. Parashar,[50] V. Parihar,[72] S. K. Park,[28] R. Partridge,[72,¶] N. Parua,[49] A. Patwa,[68] B. Penning,[45] M. Perfilov,[34] Y. Peters,[41] K. Petridis,[41] G. Petrillo,[66] P. Pétroff,[13] M.-A. Pleier,[68] P. L. M. Podesta-Lerma,[29,§§] V. M. Podstavkov,[45] P. Polozov,[33] A. V. Popov,[35] M. Prewitt,[75] D. Price,[49] N. Prokopenko,[35] J. Qian,[58] A. Quadt,[20] B. Quinn,[60] M. S. Rangel,[1] K. Ranjan,[25] P. N. Ratoff,[39] I. Razumov,[35] P. Renkel,[74] I. Ripp-Baudot,[16] F. Rizatdinova,[71] M. Rominsky,[45] A. Ross,[39] C. Royon,[15] P. Rubinov,[45] R. Ruchti,[51] G. Safronov,[33] G. Sajot,[11] P. Salcido,[47] A. Sánchez-Hernández,[29] M. P. Sanders,[22] B. Sanghi,[45] A. S. Santos,[1,‖‖] G. Savage,[45] L. Sawyer,[55] T. Scanlon,[40] R. D. Schamberger,[67] Y. Scheglov,[36] H. Schellman,[48] S. Schlobohm,[77] C. Schwanenberger,[41] R. Schwienhorst,[59] J. Sekaric,[53] H. Severini,[70] E. Shabalina,[20] V. Shary,[15] S. Shaw,[59] A. A. Shchukin,[35] R. K. Shivpuri,[25] V. Simak,[7] P. Skubic,[70] P. Slattery,[66] D. Smirnov,[51] K. J. Smith,[64] G. R. Snow,[61] J. Snow,[69] S. Snyder,[68] S. Söldner-Rembold,[41] L. Sonnenschein,[18] K. Soustruznik,[6] J. Stark,[11] V. Stolin,[33] D. A. Stoyanova,[35] M. Strauss,[70] L. Stutte,[45] L. Suter,[41] P. Svoisky,[70] M. Takahashi,[41] M. Titov,[15] V. V. Tokmenin,[32] Y.-T. Tsai,[66] K. Tschann-Grimm,[67] D. Tsybychev,[67] B. Tuchming,[15] C. Tully,[63] L. Uvarov,[36] S. Uvarov,[36] S. Uzunyan,[47] R. Van Kooten,[49] W. M. van Leeuwen,[30] N. Varelas,[46] E. W. Varnes,[42] I. A. Vasilyev,[35] P. Verdier,[17] A. Y. Verkheev,[32] L. S. Vertogradov,[32] M. Verzocchi,[45] M. Vesterinen,[41] D. Vilanova,[15] P. Vokac,[7] H. D. Wahl,[44] M. H. L. S. Wang,[45] J. Warchol,[51] G. Watts,[77] M. Wayne,[51] J. Weichert,[21] L. Welty-Rieger,[48] A. White,[73] D. Wicke,[23] M. R. J. Williams,[39] G. W. Wilson,[53] M. Wobisch,[55] D. R. Wood,[57]

T. R. Wyatt,[41] Y. Xie,[45] S. Yacoob,[48,¶¶] R. Yamada,[45] W.-C. Yang,[41] T. Yasuda,[45] Y. A. Yatsunenko,[32] W. Ye,[67] Z. Ye,[45] H. Yin,[45] K. Yip,[68] S. W. Youn,[45] T. Zhao,[77] T. G. Zhao,[41] B. Zhou,[58] J. Zhu,[58] M. Zielinski,[66] D. Zieminska,[49] and L. Zivkovic[72]

(D0 Collaboration)

[1]*LAFEX, Centro Brasileiro de Pesquisas Físicas, Rio de Janeiro, Brazil*
[2]*Universidade do Estado do Rio de Janeiro, Rio de Janeiro, Brazil*
[3]*Universidade Federal do ABC, Santo André, Brazil*
[4]*University of Science and Technology of China, Hefei, People's Republic of China*
[5]*Universidad de los Andes, Bogotá, Colombia*
[6]*Faculty of Mathematics and Physics, Center for Particle Physics, Charles University, Prague, Czech Republic*
[7]*Czech Technical University in Prague, Prague, Czech Republic*
[8]*Center for Particle Physics, Institute of Physics, Academy of Sciences of the Czech Republic, Prague, Czech Republic*
[9]*Universidad San Francisco de Quito, Quito, Ecuador*
[10]*LPC, Université Blaise Pascal, CNRS/IN2P3, Clermont, France*
[11]*LPSC, Université Joseph Fourier Grenoble 1, CNRS/IN2P3, Institut National Polytechnique de Grenoble, Grenoble, France*
[12]*CPPM, Aix-Marseille Université, CNRS/IN2P3, Marseille, France*
[13]*LAL, Université Paris-Sud, CNRS/IN2P3, Orsay, France*
[14]*LPNHE, Universités Paris VI and VII, CNRS/IN2P3, Paris, France*
[15]*CEA, Irfu, SPP, Saclay, France*
[16]*IPHC, Université de Strasbourg, CNRS/IN2P3, Strasbourg, France*
[17]*IPNL, Université Lyon 1, CNRS/IN2P3, Villeurbanne, France and Université de Lyon, Lyon, France*
[18]*III. Physikalisches Institut A, RWTH Aachen University, Aachen, Germany*
[19]*Physikalisches Institut, Universität Freiburg, Freiburg, Germany*
[20]*II. Physikalisches Institut, Georg-August-Universität Göttingen, Göttingen, Germany*
[21]*Institut für Physik, Universität Mainz, Mainz, Germany*
[22]*Ludwig-Maximilians-Universität München, München, Germany*
[23]*Fachbereich Physik, Bergische Universität Wuppertal, Wuppertal, Germany*
[24]*Panjab University, Chandigarh, India*
[25]*Delhi University, Delhi, India*
[26]*Tata Institute of Fundamental Research, Mumbai, India*
[27]*University College Dublin, Dublin, Ireland*
[28]*Korea Detector Laboratory, Korea University, Seoul, Korea*
[29]*CINVESTAV, Mexico City, Mexico*
[30]*Nikhef, Science Park, Amsterdam, the Netherlands*
[31]*Radboud University Nijmegen, Nijmegen, the Netherlands*
[32]*Joint Institute for Nuclear Research, Dubna, Russia*
[33]*Institute for Theoretical and Experimental Physics, Moscow, Russia*
[34]*Moscow State University, Moscow, Russia*
[35]*Institute for High Energy Physics, Protvino, Russia*
[36]*Petersburg Nuclear Physics Institute, St. Petersburg, Russia*
[37]*Institució Catalana de Recerca i Estudis Avançats (ICREA) and Institut de Física d'Altes Energies (IFAE), Barcelona, Spain*
[38]*Stockholm University, Stockholm and Uppsala University, Uppsala, Sweden*
[39]*Lancaster University, Lancaster LA1 4YB, United Kingdom*
[40]*Imperial College London, London SW7 2AZ, United Kingdom*
[41]*The University of Manchester, Manchester M13 9PL, United Kingdom*
[42]*University of Arizona, Tucson, Arizona 85721, USA*
[43]*University of California Riverside, Riverside, California 92521, USA*
[44]*Florida State University, Tallahassee, Florida 32306, USA*
[45]*Fermi National Accelerator Laboratory, Batavia, Illinois 60510, USA*
[46]*University of Illinois at Chicago, Chicago, Illinois 60607, USA*
[47]*Northern Illinois University, DeKalb, Illinois 60115, USA*
[48]*Northwestern University, Evanston, Illinois 60208, USA*
[49]*Indiana University, Bloomington, Indiana 47405, USA*
[50]*Purdue University Calumet, Hammond, Indiana 46323, USA*
[51]*University of Notre Dame, Notre Dame, Indiana 46556, USA*
[52]*Iowa State University, Ames, Iowa 50011, USA*
[53]*University of Kansas, Lawrence, Kansas 66045, USA*

[54]Kansas State University, Manhattan, Kansas 66506, USA
[55]Louisiana Tech University, Ruston, Louisiana 71272, USA
[56]Boston University, Boston, Massachusetts 02215, USA
[57]Northeastern University, Boston, Massachusetts 02115, USA
[58]University of Michigan, Ann Arbor, Michigan 48109, USA
[59]Michigan State University, East Lansing, Michigan 48824, USA
[60]University of Mississippi, University, Mississippi 38677, USA
[61]University of Nebraska, Lincoln, Nebraska 68588, USA
[62]Rutgers University, Piscataway, New Jersey 08855, USA
[63]Princeton University, Princeton, New Jersey 08544, USA
[64]State University of New York, Buffalo, New York 14260, USA
[65]Columbia University, New York, New York 10027, USA
[66]University of Rochester, Rochester, New York 14627, USA
[67]State University of New York, Stony Brook, New York 11794, USA
[68]Brookhaven National Laboratory, Upton, New York 11973, USA
[69]Langston University, Langston, Oklahoma 73050, USA
[70]University of Oklahoma, Norman, Oklahoma 73019, USA
[71]Oklahoma State University, Stillwater, Oklahoma 74078, USA
[72]Brown University, Providence, Rhode Island 02912, USA
[73]University of Texas, Arlington, Texas 76019, USA
[74]Southern Methodist University, Dallas, Texas 75275, USA
[75]Rice University, Houston, Texas 77005, USA
[76]University of Virginia, Charlottesville, Virginia 22901, USA
[77]University of Washington, Seattle, Washington 98195, USA
(Received 1 March 2012; published 12 April 2012)

We present a measurement of the W boson mass using data corresponding to 4.3 fb^{-1} of integrated luminosity collected with the D0 detector during Run II at the Fermilab Tevatron $p\bar{p}$ collider. With a sample of 1 677 394 $W \to e\nu$ candidate events, we measure $M_W = 80.367 \pm 0.026$ GeV. This result is combined with an earlier D0 result determined using an independent Run II data sample, corresponding to 1 fb^{-1} of integrated luminosity, to yield $M_W = 80.375 \pm 0.023$ GeV.

DOI: 10.1103/PhysRevLett.108.151804 PACS numbers: 14.70.Fm, 12.15.Ji, 13.38.Be, 13.85.Qk

In the context of the standard model (SM), there is a relationship between the W boson mass (M_W) and the hypothetical Higgs boson mass (and other observables such as the top quark mass). Accurate measurement of the M_W is thus a key ingredient in constraining the SM Higgs boson mass and comparing that constraint with the results of direct Higgs boson searches. Precise measurements of M_W have been reported by the ALEPH [1], DELPHI [2], L3 [3], OPAL [4], D0 [5,6], and CDF [7,8] collaborations. The W boson mass experimental methods and measurements are discussed in Ref. [9]. The current world average measured value is $M_W = 80.399 \pm 0.023$ GeV [10]. This result and the current measurement [11] of the top quark mass, M_t, give a range for the predicted M_H which is centered on a value outside the direct search allowed range. The predicted range is, however, large and does have some overlap with the regions allowed by direct searches. The limiting factor in the predictions is the experimental precision on M_W. It is therefore of great interest to improve the precision of the W boson mass measurement so as to further probe the validity of the SM.

In this Letter, we present a measurement of M_W using data collected from 2006 to 2009 with the D0 detector [12], corresponding to a total integrated luminosity of 4.3 fb^{-1}. We use the $W \to e\nu$ decay mode because the D0 calorimeter is well suited for a precise measurement of electron [13] energies. For the data considered in this analysis, the average energy resolution is 4.2% for electrons of 45 GeV. The longitudinal components of the colliding partons and of the neutrino cannot be determined, so M_W is determined using three kinematic variables measured in the plane perpendicular to the beam direction: the transverse mass m_T, the electron transverse momentum p_T^e, and the neutrino transverse momentum p_T^ν. The transverse mass is defined as $m_T = \sqrt{2 p_T^e p_T^\nu (1 - \cos\Delta\phi)}$, where $\Delta\phi$ is the opening angle between the electron and neutrino momenta in the plane transverse to the beam. The vector $\vec{p}_T^{\,\nu}$ is equal to the event missing transverse momentum ($\vec{\not\!\!E}_T$).

The D0 detector [12] comprises a tracking system, calorimeters and a muon system with an iron toroid magnet. Silicon microstrip tracking detectors (SMT) near the interaction point cover $|\eta| < 3$, where $\eta \equiv -\ln[\tan(\theta/2)]$ and θ is the polar angle with respect to the proton beam direction, to provide tracking and vertex information. The central fiber tracker surrounds the SMT, providing coverage to $|\eta| \approx 2$. A 1.9 T solenoid surrounds these tracking detectors. Three uranium liquid-argon calorimeters measure particle energies. The central calorimeter (CC) covers $|\eta| < 1.1$, and two end calorimeters (EC) extend coverage to $|\eta| \approx 4$. The CC is segmented in depth into eight layers. The first four layers allow for a precise measurement of the energy of photons and electrons. The remaining four layers, along with the first four, are used to measure the energy of hadrons. A three-level trigger system selects events for recording with a rate of ≈ 100 Hz.

The present analysis builds on the techniques developed in Ref. [6]. Additional studies are necessary to cope with the consequences of the increased instantaneous luminosities (on average 1.2×10^{32} cm^{-2} S^{-1}, almost 3 times higher than in Ref. [6]). The main developments include a new model of dependence of the gains of the D0 calorimeter on the instantaneous luminosity. This dependence had been predicted [14] before the start of Run II and has been studied in detail in the data used for this Letter. The other important additions are a correction for residual η-dependent miscalibrations of the calorimeter response, a more detailed model of the impact of additional $p\bar{p}$ interactions on the electron energy reconstruction, and a detailed description of electron efficiency in the presence of additional $p\bar{p}$ interactions. Using the same method as Ref. [6] we obtain the amount of material preceding the calorimeter from a fit to the longitudinal energy profile in the electromagnetic calorimeter.

Events are selected using a trigger requiring at least one electromagnetic (EM) cluster found in the CC with the transverse energy threshold varying from 25 to 27 GeV depending on run conditions. The offline selection of candidate W boson events is similar to that used in Ref. [6], except that the veto on electrons in ϕ regions with degraded energy response is now based on extrapolation of the track to the third calorimeter layer instead of the position of the calorimeter cluster. We require at least one candidate electron reconstructed as an EM cluster in the CC, matched in (η, ϕ) space to a track including at least one SMT hit and $p_T > 10$ GeV to reject jets misidentified as electrons and to ensure a precise measurement of the electron direction. The length of the electron three-momentum vector is defined by the cluster energy, and the direction by the track. We require an electron with $p_T^e > 25$ GeV that passes shower shape and isolation requirements and points to the central 80% in azimuth of a CC ($|\eta| < 1.05$) module. The event must satisfy $\not{E}_T > 25$ GeV, $u_T < 15$ GeV, and $50 < m_T < 200$ GeV. Here u_T is the magnitude of the vector sum of the transverse component of the energies measured in calorimeter cells excluding those associated with the reconstructed electron. The relation $\vec{\not{E}}_T = -(\vec{p}_T^{\,e} + \vec{u}_T)$ defines the missing momentum ascribed to the neutrino. This selection yields 1 677 394 candidate $W \to e\nu$ events.

Candidate $Z \to ee$ events are required to have two EM clusters satisfying the above requirements, except that one of the two may be reconstructed within an EC ($1.5 < |\eta| < 2.5$). The associated tracks must be of opposite curvature. Events must also have $u_T < 15$ GeV and $70 \le m_{ee} \le 110$ GeV, where m_{ee} is the invariant mass of the electron pair. Events with both electrons in the CC are used to determine the calibration of the electron energy scale. There are 54 512 candidate $Z \to ee$ events in this category. Events with one electron in EC are only used for the efficiency measurement.

The backgrounds in the W boson candidate sample are $Z \to ee$ events where one electron escapes detection, multijet events where a jet is misidentified as an electron with $\not{E}_T$ arising from misreconstruction, and $W \to \tau\nu \to e\nu\nu\nu$ events. The backgrounds are estimated using refined versions of the techniques in Ref. [6], and their impact on the measurement of M_W is small. The fractions of the backgrounds in the W boson candidate sample are 1.08% for $Z \to ee$, 1.02% for multijet events, and 1.67% for $W \to \tau\nu \to e\nu\nu\nu$.

The RESBOS [15] event generator, combined with PHOTOS [16] is used to simulate the kinematics of W and Z boson production and decay. RESBOS is a next-to-leading order event generator including next-to-next-to-leading logarithm resummation of soft gluons [17], and PHOTOS generates up to two final state radiation photons. Parton distribution functions (PDF) are described using CTEQ6.6 [18]. This combination provides a good description of the most important effects in the M_W measurement, namely, the boson transverse momentum spectrum (influenced by the emission of multiple soft gluons) and radiation from the electrons in the final state. We use comparisons to the WGRAD [19] and ZGRAD [20] event generators, which provide a more complete treatment of electroweak corrections at the one radiated photon level, in order to assess the uncertainty in the M_W measurement due to quantum electrodynamics (QED) corrections. We take the nonperturbative parameter g_2 [21] to be 0.68 ± 0.02 GeV^2 [22] and the uncertainty on g_2 is propagated to the W boson mass uncertainty.

A fast, parametrized Monte Carlo (MC) simulation (FASTMC) is used to simulate electron identification efficiencies and the energy response and resolutions of the electron and recoil system in the generated events. The FASTMC parameters are determined using a combination of detailed simulation and control data samples. The primary control sample used for both the electromagnetic and hadronic response tuning is $Z \to ee$ events. Events recorded in random beam crossings are overlaid on W and Z events in the detailed simulation to quantify the effect of additional collisions in the same or nearby bunch crossings.

The Z boson mass and width are known with high precision from measurements at LEP [23]. These values are used to calibrate the electromagnetic calorimeter response assuming a form $E^{\mathrm{meas}} = \alpha E^{\mathrm{true}} + \beta$ with constants α and β determined from fits to the dielectron mass spectrum and the energy and angular distributions of the two electrons. The M_W measurement presented here is effectively a measurement of the ratio of W and Z boson masses.

The hadronic energy in the event contains the hadronic system recoiling from the W boson, the effects of low energy products from spectator parton collisions and other beam collisions, final state radiation, and energy from the recoil particles that enter the electron selection window. The hadronic response (resolution) is calibrated using the mean (width) of the $\eta_{\rm imb}$ distribution in $Z \to ee$ events in bins of p_T^{ee}. Here, $\eta_{\rm imb}$ is defined as the projections of the sum of dielectron transverse momentum ($\vec{p}_T^{ee}$) and $\vec{u}_T$ vectors on the axis bisecting the dielectron directions in the transverse plane [24].

The combination of event generator and FASTMC is used to predict the shapes of m_T, p_T^e, and $\not\!\!E_T$ for a given M_W hypothesis. M_W is determined separately for each of the three observables by maximizing a binned likelihood between the data distribution and the predicted distribution normalized to the data. The fit ranges are optimized as indicated in Table I.

A test of the analysis procedure is performed using $W \to e\nu$ events, generated by the PYTHIA [25] event generator and processed through a detailed GEANT MC simulation [26], which are treated as collider data. The FASTMC is separately tuned to give agreement with the GEANT events in the same way as for the data comparison. Each of the M_W fit results using the m_T, p_T^e, and $\not\!\!E_T$ distributions agree with the input M_W value within the 6 MeV total uncertainty of the test arising from MC statistics.

During the FASTMC tuning performed to describe the collider data, the M_W values returned from fits had an unknown constant offset added. The same offset was used for m_T, p_T^e, and $\not\!\!E_T$. This allowed the full tuning on the W and Z boson events and internal consistency checks to be performed without knowledge of the final result. Once the important data and FASTMC comparison plots had acceptable χ^2 distributions, the common offset was removed from the results. The Z boson mass from the fit to the data corresponds to the input that was used in the determination of the calorimeter response described above. The statistical uncertainty from the fit is 0.017 GeV, quoted here as a quantitative illustration of the statistical power of the $Z \to ee$ sample. Figure 1 shows a comparison of the m_{ee} distributions for data and FASTMC. The M_W results are given in Table I. The m_T, p_T^e, and $\not\!\!E_T$ distributions showing the data and FASTMC templates with background for the best fit M_W are shown in Fig. 2.

TABLE I. Results from the fits to data. The uncertainty is solely due to the statistics of the W boson sample.

Variable	Fit Range (GeV)	M_W(GeV)	χ^2/dof
m_T	$65 < m_T < 90$	80.371 ± 0.013	37.4/49
p_T^e	$32 < p_T^e < 48$	80.343 ± 0.014	26.7/31
$\not\!\!E_T$	$32 < \not\!\!E_T < 48$	80.355 ± 0.015	29.4/31

The systematic uncertainties in the M_W measurement are summarized in Table II. They can be categorized as those from experimental sources and those from uncertainties in the production mechanism. The uncertainties on the electron energy calibration, the electron energy resolution, and the hadronic recoil model arise from the finite size of the $Z \to ee$ sample used to derive them. The uncertainties in the propagation of electron energy calibrations from the $Z \to ee$ to the $W \to e\nu$ sample are determined by the difference in energy loss in the uninstrumented material in front of the calorimeter. The energy loss as a function of electron energy and η is derived from a dedicated detailed GEANT simulation of the D0 detector. The shower modeling systematic uncertainties reflect the uncertainties in the amount of uninstrumented material, and the energy loss systematic uncertainties arise from the finite precision of our simulations of electron showers based on a detailed model of the detector geometry. The systematic uncertainties of electron efficiency, hadronic recoil model, and backgrounds are determined by varying the corresponding parameters within the statistical uncertainties of their measurements. Table II also shows the M_W uncertainties arising from the backgrounds.

The uncertainties due to the production mechanism are dominated by the uncertainties due to the PDFs. The transverse observables (m_T, p_T^e, and $\not\!\!E_T$) used in the measurement of M_W are invariant under longitudinal boosts, and their use therefore minimizes the sensitivity to PDF uncertainties. However, a limited sensitivity to PDF uncertainties does arise from the electron pseudorapidity requirements that are used in the measurement of M_W reported here. These requirements are not invariant under longitudinal boosts, and changes in the PDF can therefore

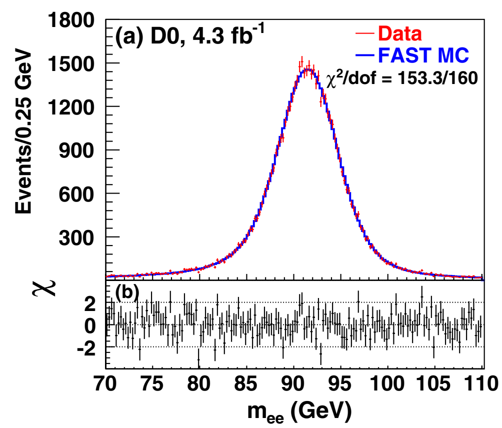

FIG. 1 (color online). (a) The dielectron invariant mass distribution in $Z \to ee$ data and from the FASTMC and (b) the χ values, where $\chi_i = [N_i - (\text{FASTMC}_i)]/\sigma_i$ for each bin in the distribution, N_i and FASTMC$_i$ are the data and FASTMC template yields in bin i, respectively, and σ_i is the statistical uncertainty in bin i.

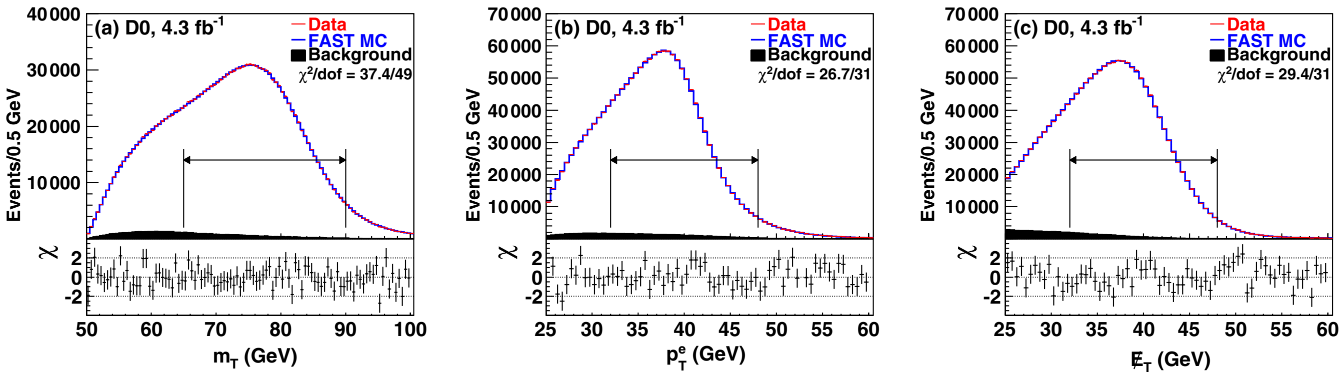

FIG. 2 (color online). The (a) m_T, (b) p_T^e, and (c) $\not\!\!E_T$ distributions for data and FASTMC simulation with backgrounds. The χ values are shown below each distribution, where $\chi_i = [N_i - (\text{FASTMC}_i)]/\sigma_i$ for each bin in the distribution, N_i and FASTMC$_i$ are the data and FASTMC template yields in bin i, respectively, and σ_i is the statistical uncertainty in bin i. The fit ranges are indicated by the double-ended horizontal arrows.

result in changes of the shapes of our transverse observables. The uncertainties in the PDF are propagated to a 1 standard deviation uncertainty in M_W by generating ensembles of W boson events using PYTHIA with the CTEQ6.1 [27] prescription. The other production uncertainties have been discussed above.

The quality of the simulation is indicated by the χ^2 values computed for the differences between the data and FASTMC shown in Figs. 1 and 2. We perform a variety of consistency checks of the stability of our results. We vary the fit ranges for the m_T, p_T^e, and $\not\!\!E_T$ distributions. The data are also divided into statistically independent categories based on instantaneous luminosity, time, electron η, and the projection of $\vec{u}_T$ on the electron direction. The exclusion region near CC module edges is varied, and the selection requirement on u_T is varied. The results are stable to within the measurement uncertainty for each of these tests.

The total correlations among the three W boson mass measurements are determined by combining the covariance matrices for each source of uncertainty. For uncertainties which arise from sample statistics, such as the electron energy scale, the full covariance matrices are determined using ensemble studies. For uncertainties which are nonstatistical in nature, such as the QED uncertainty, the correlations among the three observables are defined as 100% to prevent these uncertainties from being decreased in the combination. The resulting total correlations, including both categories of uncertainties, are 0.89 (m_T, p_T^e), 0.86 (m_T, $\not\!\!E_T$), and 0.75 (p_T^e, $\not\!\!E_T$). When considering only the uncertainties which are allowed to decrease in the combination, we find that the $\not\!\!E_T$ measurement has negligible weight. We therefore combine the m_T and p_T^e measurements using the method [28] and obtain

$$M_W = 80.367 \pm 0.013(\text{stat.}) \pm 0.022(\text{syst.})\ \text{GeV}$$
$$= 80.367 \pm 0.026\ \text{GeV}.$$

The probability to observe a larger difference than observed between these two measurements is 2.8%. The probability to observe a larger difference than observed when all three measurements are combined is 5%. We combine this measurement with the earlier D0 measurement [6] to obtain

$$M_W = 80.375 \pm 0.011(\text{stat.}) \pm 0.020(\text{syst.})\ \text{GeV}$$
$$= 80.375 \pm 0.023\ \text{GeV}.$$

The dominant uncertainties arise from the available statistics of the $W \to e\nu$ and $Z \to ee$ samples. Thus, a future measurement with the full D0 data set is expected to be more precise. The M_W measurement reported here agrees with the world average [10,29] and the previous individual measurements and has an uncertainty that significantly improves upon previous D0 measurements. Our new measurement of M_W and the most recent world average measurement of M_t are compared in Fig. 3 with the regions that are still allowed, at the 95% C.L., after direct searches for the Higgs boson at LEP, the Tevatron, and the

TABLE II. Systematic uncertainties of the M_W measurement.

Source	ΔM_W(MeV) m_T	p_T^e	$\not\!\!E_T$
Electron energy calibration	16	17	16
Electron resolution model	2	2	3
Electron shower modeling	4	6	7
Electron energy loss model	4	4	4
Hadronic recoil model	5	6	14
Electron efficiencies	1	3	5
Backgrounds	2	2	2
Experimental subtotal	18	20	24
PDF	11	11	14
QED	7	7	9
Boson p_T	2	5	2
Production subtotal	13	14	17
Total	22	24	29

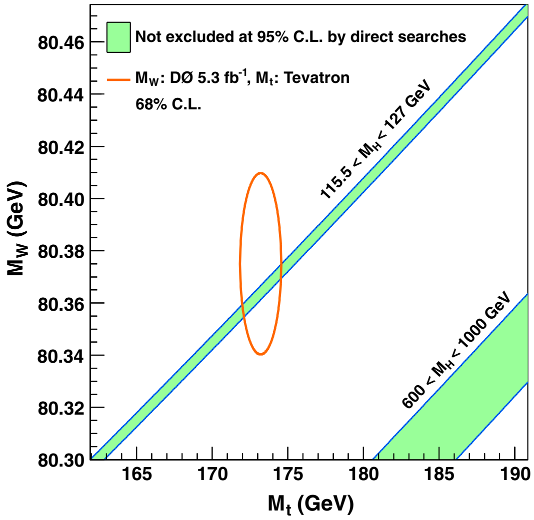

FIG. 3 (color online). Contour curves of 68% probability in the (M_t, M_W) plane. The ellipse represents the measurement of M_t from Ref. [11] and the measurement of $M_W = 80.375 \pm 0.023$ GeV reported in this Letter. The bands show the SM prediction for different Higgs boson mass hypotheses that are not yet ruled out by direct searches [30] for the Higgs boson.

LHC. Our new measurement of M_W is in good agreement with one of the regions allowed by direct searches for the Higgs boson.

We thank the staffs at Fermilab and collaborating institutions, and acknowledge support from the DOE and NSF (USA); CEA, CNRS/IN2P3 and the CIMENT project, Grenoble (France); MON, Rosatom and RFBR (Russia); CNPq, FAPERJ, FAPESP and FUNDUNESP (Brazil); DAE and DST (India); Colciencias (Colombia); CONACyT (Mexico); NRF (Korea); FOM (The Netherlands); STFC and the Royal Society (United Kingdom); MSMT and GACR (Czech Republic); BMBF and DFG (Germany); SFI (Ireland); The Swedish Research Council (Sweden); and CAS and CNSF (China).

*Deceased.
†Visitor from Augustana College, Sioux Falls, SD, USA.
‡Visitor from The University of Liverpool, Liverpool, UK.
§Visitor from UPIITA-IPN, Mexico City, Mexico.
‖Visitor from DESY, Hamburg, Germany.
¶Visitor from SLAC, Menlo Park, CA, USA.
**Visitor from University College London, London, UK.
††Visitor from Centro de Investigacion en Computacion-IPN, Mexico City, Mexico.
‡‡Visitor from Thomas Jefferson National Accelerator Facility (JLab), Newport News, VA, USA.
§§Visitor from ECFM, Universidad Autonoma de Sinaloa, Culiacán, Mexico.
‖‖Visitor from Universidade Estadual Paulista, São Paulo, Brazil.
¶¶Visitor from School of Physics, University of the Witwatersrand, Johannesburg, South Africa.

[1] S. Schael *et al.* (ALEPH Collaboration), Eur. Phys. J. C **47**, 309 (2006).
[2] J. Abdallah *et al.* (DELPHI Collaboration), Eur. Phys. J. C **55**, 1 (2008).
[3] P. Achard *et al.* (L3 Collaboration), Eur. Phys. J. C **45**, 569 (2006).
[4] G. Abbiendi *et al.* (OPAL Collaboration), Eur. Phys. J. C **45**, 307 (2005).
[5] B. Abbott *et al.* (D0 Collaboration), Phys. Rev. D **58**, 092003 (1998); B. Abbott *et al.* (D0 Collaboration), Phys. Rev. D **62**, 092006 (2000); V. M. Abazov *et al.* (D0 Collaboration), Phys. Rev. D **66**, 012001 (2002).
[6] V. M. Abazov *et al.* (D0 Collaboration), Phys. Rev. Lett. **103**, 141801 (2009).
[7] T. Affolder *et al.* (CDF Collaboration), Phys. Rev. D **64**, 052001 (2001).
[8] T. Aaltonen *et al.* (CDF Collaboration), Phys. Rev. Lett. **99**, 151801 (2007); T. Aaltonen *et al.* (CDF Collaboration), Phys. Rev. D **77**, 112001 (2008).
[9] A. V. Kotwal and J. Stark, Annu. Rev. Nucl. Part. Sci. **58**, 147 (2008).
[10] LEP Electroweak Working Group and Tevatron Electroweak Working Group, CERN Report No. CERN-PH-EP-2010-095, and Fermilab Report No. FERMILAB-TM-2480-PPD, 2010, arXiv:1012.2367.
[11] Tevatron Electroweak Working Group, CDF and D0 Collaborations, arXiv:1107.5255.
[12] V. M. Abazov *et al.* (D0 Collaboration), Nucl. Instrum. Methods Phys. Res., Sect. A **565**, 463 (2006).
[13] Throughout this Letter we use electron to imply either electron or positron.
[14] H. Montgomery *et al.* (D0 Collaboration), arXiv:hep-ex/9804011.
[15] C. Balazs and C. P. Yuan, Phys. Rev. D **56**, 5558 (1997).
[16] P. Golonka and Z. Was, Eur. Phys. J. C **45**, 97 (2006).
[17] J. C. Collins, D. E. Soper, and G. Sterman, Nucl. Phys. **B250**, 199 (1985).
[18] P. M. Nadolsky, H.-L. Lai, Q.-H. Cao, J. Huston, J. Pumplin, D. Stump, W.-K. Tung, and C.-P. Yuan, Phys. Rev. D **78**, 013004 (2008).
[19] U. Baur, S. Keller, and D. Wackeroth, Phys. Rev. D **59**, 013002 (1998).
[20] U. Baur, S. Keller, and W. K. Sakumoto, Phys. Rev. D **57**, 199 (1998); U. Baur, O. Brein, W. Hollik, C. Schappacher, and D. Wackeroth, Phys. Rev. D **65**, 033007 (2002).
[21] F. Landry, R. Brock, P. M. Nadolsky, and C. P. Yuan, Phys. Rev. D **67**, 073016 (2003).
[22] V. M. Abazov *et al.* (D0 Collaboration), Phys. Rev. Lett. **100**, 102002 (2008).
[23] ALEPH Collaboration, DELPHI Collaboration, L3 Collaboration, OPAL Collaboration, SLD Collaboration, LEP Electroweak Working Group, and SLD Electroweak and Heavy Flavour Groups, Phys. Rep. **427**, 257 (2006).
[24] J. Alitti *et al.* (UA2 Collaboration), Phys. Lett. B **276**, 354 (1992).

[25] T. Sjöstrand, S. Mrenna, and P. Skands, J. High Energy Phys. 05 (2006) 026.
[26] R. Brun and F. Carminati, CERN Program Library Long Writeup, Report No. W5013, 1993.
[27] H. L. Lai, J. Huston, S. Kuhlmann, F. Olness, J. Owens, D. Soper, W. K. Tung, and H. Weerts, Phys. Rev. D **55**, 1280 (1997); D. Stump, J. Huston, J. Pumplin, W.-K. Tung, H.-L. Lai, S. Kuhlmann, and J. F. Owens, J. High Energy Phys. 10 (2003) 046.
[28] L. Lyons, D. Gibout, and P. Clifford, Nucl. Instrum. Methods Phys. Res., Sect. A **270**, 110 (1988); A. Valassi, Nucl. Instrum. Methods Phys. Res., Sect. A **500**, 391 (2003).
[29] RESBOS uses a W width of 2100.4 MeV. Combinations [10] normally use a standard model width of 2093.2 ± 2.2 MeV (using the current world average m_W), which would require a correction of 1.1 ± 0.5 MeV to our quoted result.
[30] G. Abbiendi *et al.* (ALEPH Collaboration, DELPHI Collaboration, L3 Collaboration, OPAL Collaboration, and LEP Working Group for Higgs Boson Searches), Phys. Lett. B **565**, 61 (2003); Tevatron New Phenomena and Higgs Working Group, CDF, and D0 collaborations, arXiv:1203.3774; G. Aad *et al.* (ATLAS Collaboration), Phys. Lett. B **710**, 49 (2012); S. Chatrchyan *et al.* (CMS Collaboration), Phys. Lett. B **710**, 26 (2012).